

Nonlinear Optical Studies on New Conjugated Poly{2,2¹-(3,4-dialkoxythiophene-2,5-diyl)bis[5-(2-thienyl)-1,3,4-oxadiazole]}s

Pramod Kumar Hegde,¹ A. Vasudeva Adhikari,¹ M. G. Manjunatha,^{1*} C. S. Suchand Sandeep,² Reji Philip²

¹Organic Chemistry Division, Department of Chemistry, National Institute of Technology Karnataka, Surathkal, Mangalore 575025, India

²Light and Matter Physics Group, Raman Research Institute, Bangalore 560080, India

Received 30 September 2008; accepted 28 May 2009

DOI 10.1002/app.30926

Published online 27 April 2010 in Wiley InterScience (www.interscience.wiley.com).

ABSTRACT: Three new donor–acceptor type poly{2,2¹-(3,4-dialkoxythiophene-2,5-diyl)bis[5-(2-thienyl)-1,3,4-oxadiazole]}s (**P1**, **P2**, and **P3**) were synthesized starting from thiodiglycolic acid and diethyl oxalate through multistep reactions. The polymerization was carried out using chemical polymerization technique. The optical and charge-transporting properties of the polymers were investigated by UV-visible, fluorescence emission spectroscopic and cyclic voltammetric studies. The polymers showed bluish-green fluorescence in solutions. The electrochemical band gaps were determined to be 2.03, 2.09, and 2.17 eV for **P1**, **P2**, and **P3**, respectively. The nonlinear optical

properties of new polymers were investigated at 532 nm using single beam Z-scan and degenerate four-wave mixing (DFWM) techniques with nanosecond laser pulses. The polymers exhibited strong optical limiting behavior due to “effective” three-photon absorption. Values of the effective three-photon absorption (3PA) coefficients, third-order nonlinear susceptibilities ($\chi^{(3)}$), and figures (F) of merit were calculated. © 2010 Wiley Periodicals, Inc. *J Appl Polym Sci* 117: 2641–2650, 2010

Key words: conjugated polymer; synthesis; 3,4-dialkoxythiophene; NLO; 3PA

INTRODUCTION

Nonlinear optics (NLO) has received considerable attention due to its potential applications in optical switching, optical data storage, optical communications, and eye and sensor protection.^{1–3} A wide category of materials have been investigated for NLO properties, in which organic materials are attractive mainly due to their large variety, high nonlinearity, ultra-fast response and flexibility they offer to tune the optical properties. Recently, conjugated polymeric systems have emerged as a promising class of NLO materials, characterized by large third-order susceptibility along the directions of polymer chain. These macromolecules offer good flexibility, at both molecular and bulk levels for structural modifications that are necessary to optimize them for specific device applications. As the nonlinear response of these systems is determined primarily by their

chemical structure, one can design the unique molecular structure and synthesize compounds with enhanced nonlinear response by introducing suitable substituent groups.

In general, presence of strong π -electron delocalization in the molecular structure, that determines the polarizability of the molecule, enhances the NLO properties. Recently, Cassano et al.⁴ reported a new strategy for tuning the linear and nonlinear optical properties of conjugated polymers. According to them, incorporation of alternate electron-acceptor and electron-donor units in the polymer backbone would enhance the NLO properties, mainly due to hyperpolarizability.

Apart from NLO properties, conjugated polymers find wide range of applications in devices, such as Optoelectronics, Light Emitting Diodes (LEDs), Field Effect Transistors, Electrochemical Cells, and Organic Photovoltaic Cells. Amongst various newly developed polymers, poly(1,4-phenylenevinylene) (PPV),⁵ poly(*p*-phenylene) (PPs),⁶ polyfluorenes (PFs),⁷ and polythiophenes (PTs)⁸ were in the focus of investigations.

Thiophene-based polymers are currently under intense investigation for third-order NLO properties mainly because of their chemical stability, easy processibility, and readiness of functionalities.^{9–11}

*Present address: Organic Chemistry Division, Department of Chemistry, National Institute of Technology Karnataka, Surathkal, Mangalore 575025, India

Correspondence to: A. V. Adhikari (avchem@nitk.ac.in or avadhikari123@yahoo.co.in).

Further, good film forming properties, solubility, and adequate mechanical properties made them better choice for device fabrication in comparison with their inorganic counterparts. In polythiophenes, nonlinear optical properties can be synthetically tuned by introducing electron releasing and electron accepting segments in the polymer chain, which would result in increased delocalization in the molecule. Following the similar strategies, Adhikari and coworkers have synthesized few donor-acceptor type polythiophenes and studied the relationship between their structure and NLO properties.¹²⁻¹⁴ According to the authors, electron releasing and electron accepting groups along the polymer backbone would be a promising molecular design for enhancing the third-order NLO properties.

In this context, it has been planned to incorporate additional two unsubstituted thiophene moieties in between 3,4-dialkoxy substituted thiophenyl oxadiazole systems in our synthetic design, to enhance electron accepting nature within the polymer chain, hoping that the resulting molecule would exhibit better NLO properties. Further, it has been predicted that the presence of unsubstituted thiophene rings reduces the steric repulsion between the bulky alkoxy groups and increases the planarity of the polymer chain that could help to reduce the band gap. In this communication, we hereby report the synthesis of hitherto unknown polymers (**P1**, **P2**, and **P3**) carrying 2,2¹-(3,4-dialkoxythiophene-2,5-diyl)bis[5-(2-thienyl)-1,3,4-oxadiazole] units and investigation of their NLO properties in detail.

EXPERIMENTAL

Materials and instrumentation

3,4-Dialkoxythiophene-2,5-dicarbohydrazides (**1a-c**) were synthesized according to the reported procedure.^{15,16} Dimethylformamide and acetonitrile were dried over CaH₂. Thiodiglycolic acid, diethyl oxalate, tetrabutylammoniumperchlorate (TBAPC), and *n*-bromoalkanes were purchased from Lanchaster (UK) and were used as received. Thiophene-2-carbonyl chloride was purchased from Aldrich and directly used. All the solvents and reagents were of analytical grade. They were purchased commercially and used without further purification. Diethyl 3,4-dialkoxythiophene-2,5-dicarboxylates were synthesized according to the reported literature procedure.¹⁷⁻¹⁹

Infrared spectra of all intermediate compounds and polymers were recorded on a Nicolet Avatar 5700 FTIR (Thermo Electron Corporation). The UV-visible and fluorescence emission spectra were measured in GBC Cintra 101 UV-visible and Perkin Elmer LS55 spectrophotometers, respectively.

¹H and ¹³C-NMR spectra were obtained with AMX 400 MHz FT-NMR spectrophotometer using TMS/solvent signal as internal reference. Mass spectra were recorded on a Jeol SX-102 (FAB) Mass Spectrometer. Elemental analyses were performed on a Flash EA1112 CHNS analyzer (Thermo Electron Corporation). The electrochemical studies of the polymers were carried out using an AUTOLAB PGSTAT30 electrochemical analyzer. Cyclic voltammograms were recorded using a three-electrode cell system, with glassy carbon button as working electrode, a platinum wire as counter electrode, and an Ag/AgCl electrode as the reference electrode. Molecular weights of the polymers were determined on Waters make Gel Permeation Chromatography (GPC) using polystyrene standards in THF solvent.

Z-scan measurement

The Z-scan is a widely used technique developed by Sheik Bahae et al.²⁰ to measure the nonlinear absorption coefficient and nonlinear refractive index of materials. The "open aperture" z-scan gives information about the nonlinear absorption coefficient. Here, a Gaussian laser beam is used for molecular excitation, and its propagation direction is taken as the z-axis. The beam is focused using a convex lens, and the focal point is taken as $z = 0$. Obviously, the beam will have maximum energy density at the focus, which will symmetrically reduce towards either side of it, for the positive and negative values of z . The experiment is done by placing the sample in the beam at different positions with respect to the focus (different values of z), and measuring the corresponding transmission. The sample sees different laser intensity at each position, and hence, its intensity-dependent transmission will be position dependent. From this information the nonlinear absorption coefficient can be calculated.

In our Z-scan setup we used a stepper motor controlled linear translation stage to move the sample through the beam in precise steps. The samples were taken in a 1 mm cuvette. The transmission of the sample at each point was measured by means of two pyroelectric energy probes (Rj7620, Laser Probe). One energy probe monitors the input energy, while the other monitors the transmitted energy through the sample. The second harmonic output (532 nm) of a Q-switched Nd:YAG laser (Quanta Ray, Spectra Physics) was used for exciting the molecules. The laser pulse width used was 7 ns. Laser pulse energy of 16 microjoules was used for the experiments. The pulses were fired in the "single shot" mode, allowing sufficient time between successive pulses to avoid accumulative thermal effects in the sample. The typical open aperture Z-scan setup is shown in Figure 1.

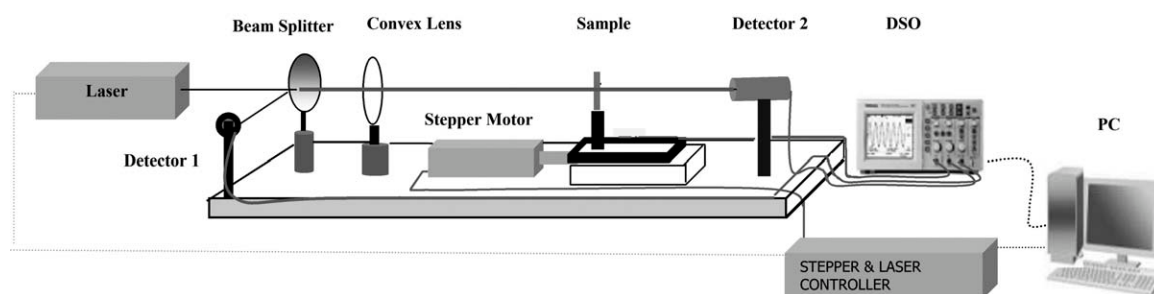


Figure 1 The open aperture Z-scan setup.

DFWM studies

Four-wave mixing refers to the interaction of four electromagnetic waves in a nonlinear optical medium via the third-order polarization. When all the waves have the same frequency, it is called degenerate four-wave mixing (DFWM). Usually, the phase-conjugate and BOXCARS geometries are used for DFWM experiments. We used the forward folded BOXCARS geometry, where a laser beam is split into three and the beams are aligned such that they form three corners of a square as shown in Figure 2. The diametrically opposite beams are the pump beams, and they have the same intensity. The third beam is the probe 3, which has an intensity of about 20% of the pump beam. When the beams are focused onto the sample the fourth beam (signal beam) is generated due to nonlinear interaction, which will appear on the fourth corner of the square. It can be measured using a detector.

In our DFWM experiment we used 7 ns pulses at 532 nm obtained from the second harmonic output of a Q-switched Nd:YAG laser. A rotating polarizer was used to change the intensity of the input laser beam. The sample was taken in a 2 mm glass cuvette. The input energy was monitored using a pyroelectric energy probe. The generated signal beam was measured in the far field using a calibrated photodiode.

Synthesis of intermediates and monomers

The intermediate 3,4-didecyloxythiophene-2,5-carboxyhydrazide (**1b**) was prepared using reported procedure.^{14,15}

General procedure for the synthesis of 3,4-dialkoxythiophene-2,5-carboxyhydrazide (1a and 1c)

Diethyl 3,4-dialkoxythiophene-2,5-dicarboxylate (0.5 g) was added into a solution of 10 mL hydrazine monohydrate in 40 mL of methanol. The reaction mixture was refluxed for 2 h. Upon cooling the solution to room temperature, a white precipitate was

obtained. The precipitate was filtered, washed with petroleum ether, dried under vacuum, and finally recrystallized from ethanol to get white solid.

3,4-Dibutoxythiophene-2,5-dicarbohydrazide (1a)

Yield; 82%, IR (cm^{-1}): 3288, 3194 (—N—H—), 3194, 2966, 2934, 2877, 1656 ($>\text{C}=\text{O}$). $^1\text{H-NMR}$ (400 MHz, CDCl_3). δ (ppm): 8.22 (s, 2H), 4.71 (s, 4H), 4.09 (t, 4H, $J = 6.9$ Hz), 1.22–1.82 (m, 8H), 0.98 (t, 6H, $J = 7.4$ Hz). Anal. Calcd. For $\text{C}_{14}\text{H}_{24}\text{N}_4\text{O}_4\text{S}$: C, 48.82; H, 7.02; N, 16.27; S, 9.31. Found: C, 48.70; H, 6.86; N, 16.10; S, 9.10.

3,4-Ditetradecyloxythiophene-2,5-dicarbohydrazide (1c)

Yield: 90%, IR (cm^{-1}): 3334, 3290 (—N—H—), 3195, 2966, 2931, 2874, 1660 ($>\text{C}=\text{O}$). $^1\text{H-NMR}$ (400 MHz, CDCl_3). δ (ppm): 8.34 (s, 2H), 4.98 (s, 4H), 4.11 (t, 4H, $J = 6.8$ Hz), 1.26–1.85 (m, 48H), 1.03 (t, 6H, $J = 7.4$ Hz). Anal. Calcd. for $\text{C}_{34}\text{H}_{64}\text{N}_4\text{O}_4\text{S}$: C, 65.34; H, 10.32; N, 8.96; S, 5.13. Found: C, 65.10; H, 10.72; N, 9.06; S, 5.00.

General procedure for the synthesis of N^2, N^5 -bis-(thiophene-2-ylcarbonyl)-3,4-dialkoxythiophene-2,5-dicarbohydrazides (3a–c)

A mixture 0.1 mol of appropriate dihydrazide (**1a,b,c**), 0.2 mol of thiophene-2-carbonyl chloride (**2**) in 20 mL of *N*-methyl pyrrolidone was taken in a round bottom flask. After adding 2 to 3 drops of

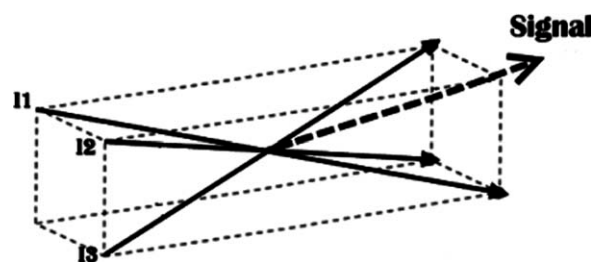


Figure 2 Four-wave mixing in the Boxcars geometry.

pyridine as catalyst, the mixture was refluxed for 10 h. The completion of the reaction was monitored by TLC. When the reaction was complete, the contents were poured into excess of water. The separated solid was filtered, washed with pet. ether (boiling range, 40–60°C), dried and recrystallized from ethanol/chloroform mixture.

*N*²,*N*⁵-Bis-(thiophene-2-ylcarbonyl)-3,4-dibutyloxythiophene-2,5-dicarbohydrazide (3a)

Yield: 80%. IR (cm⁻¹): 3235 (–N–H), 1688 (>C=O). FABHRMS: *m/z*, 564. ¹H-NMR (400 MHz, CDCl₃). δ (ppm): 10.08 (s, 2H), 9.90 (s, 2H), 7.68 (d, 2H, *J* = 3.3 Hz), 7.48 (d, 2H, *J* = 4.5 Hz), 7.02 (t, 2H, *J*₁ = 4.0 Hz, *J*₂ = 4.7 Hz), 4.16 (t, 4H, *J* = 6.9 Hz), 1.21–1.86 (m, 8H), 0.89 (t, 6H, *J* = 6.8 Hz). Anal. Calcd. for C₂₄H₂₈N₄O₆S₃: C, 51.05; H, 5.00; N, 9.92; S, 17.03. Found: C, 50.73; H, 4.68; N, 9.90; S, 16.85.

*N*²,*N*⁵-Bis-(thiophene-2-ylcarbonyl)-3,4-didecyloxythiophene-2,5-dicarbohydrazide (3b)

Yield: 80%. IR (cm⁻¹): 3228 (–N–H), 1715 (>C=O). FABHRMS: *m/z*, 732. ¹H-NMR (400 MHz, CDCl₃). δ (ppm): 10.12 (s, 2H), 9.91 (s, 2H), 7.71 (d, 2H, *J* = 3.2 Hz), 7.47 (d, 2H, *J* = 4.4 Hz), 7.04 (t, 2H, *J*₁ = 4.0 Hz, *J*₂ = 4.8 Hz), 4.26 (t, 4H, *J* = 6.8 Hz), 1.23–1.96 (m, 32H), 0.87 (t, 6H, *J* = 6.7 Hz). ¹³C-NMR (400 MHz, CDCl₃). δ (ppm): 14.10, 22.67, 25.81, 29.32, 29.35, 29.53, 29.58, 29.87, 31.86, 75.26, 123.54, 127.96, 129.62, 131.31, 135.36, 148.53, 158.91, 159.84. Anal. Calcd. for C₃₆H₅₂N₄O₆S₃: C, 58.99; H, 7.15; N, 7.64; S, 13.12. Found: C, 59.25; H, 7.34; N, 7.43; S, 13.44.

*N*²,*N*⁵-Bis-(thiophene-2-ylcarbonyl)-3,4-ditetradecyloxythiophene-2,5-dicarbohydrazide (3c)

Yield: 85%, IR (cm⁻¹): 3218 (–N–H), 1720 (>C=O). FABHRMS: *m/z*, 845. ¹H-NMR (400 MHz, CDCl₃). δ (ppm): 10.11 (s, 2H), 9.95 (s, 2H), 7.71 (d, 2H, *J* = 3.5 Hz), 7.49 (d, 2H, *J* = 4.1 Hz), 7.06 (t, 2H, *J*₁ = 4.8 Hz, *J*₂ = 3.8 Hz), 4.30 (t, 4H, *J* = 7.0 Hz), 1.24–1.96 (m, 48H), 0.88 (t, 6H, *J* = 6.5 Hz). Anal. Calcd. for C₄₄H₆₈N₄O₆S₃: C, 62.52; H, 8.11; N, 6.63; S, 11.38. Found: C, 62.88; H, 8.39; N, 6.38; S, 11.15.

General procedure for the synthesis of 2,2¹-(3,4-dialkyloxythiophene-2,5-diyl)bis[5-(2-thienyl)-1,3,4-oxadiazole] (4a–c)

A mixture of 20 mmol of biscarbohydrazide (3a–c) and 25 mL of phosphorous oxychloride were heated at 100°C for 6 h. The reaction mixture was then cooled to room temperature and poured into excess of crushed ice. The resulting precipitate was collected by filtration and washed with water followed by acetone. The crude product was dried in vacuum

oven and recrystallized with ethanol/chloroform mixture.

2,2¹-(3,4-Dibutyloxythiophene-2,5-diyl)bis[5-(2-thienyl)-1,3,4-oxadiazole] (4a)

Yield: 83%, IR (cm⁻¹): 2929, 2833, 2772, 1588 (–C=N–), 1468, 1062. FABHRMS: *m/z*, 528. ¹H-NMR (400 MHz, CDCl₃). δ (ppm): 7.75 (d, 2H, *J* = 3.9 Hz), 7.58 (d, 2H, *J* = 4.7 Hz), 7.11 (t, 2H, *J*₁ = 4.9 Hz, *J*₂ = 4.1 Hz), 4.20 (t, 4H, *J* = 6.7 Hz), 1.28–1.88 (m, 8H), 1.00 (t, 6H, *J* = 6.6 Hz). Anal. Calcd. for C₂₄H₂₄N₄O₄S₃: C, 54.53; H, 4.58; N, 10.60; S, 18.20. Found: C, 54.22; H, 4.30; N, 10.26; S, 18.48.

2,2¹-(3,4-Didecyloxythiophene-2,5-diyl)bis[5-(2-thienyl)-1,3,4-oxadiazole] (4b)

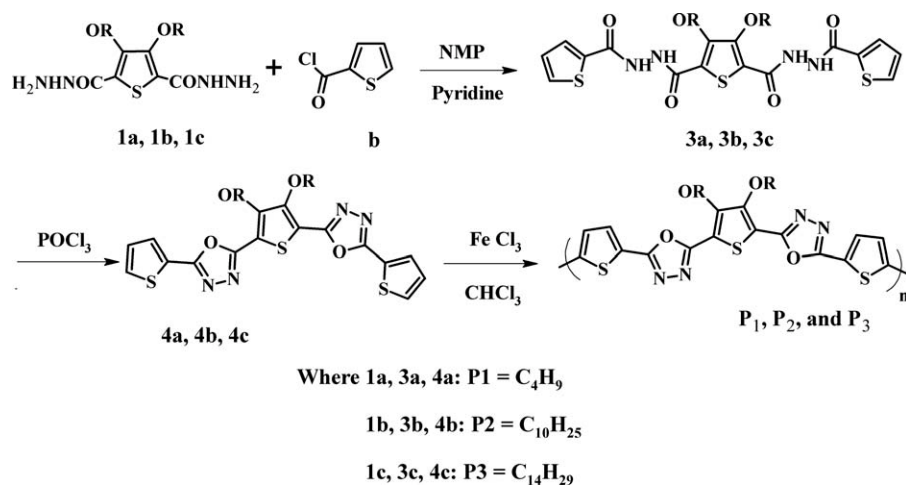
Yield: 78%, IR (cm⁻¹): 2922, 2853, 2763, 1593 (–C=N–), 1457, 1067. FABHRMS: *m/z*, 696. ¹H-NMR (400 MHz, CDCl₃). δ (ppm): 7.85 (d, 2H, *J* = 3.8 Hz), 7.61 (d, 2H, *J* = 4.8 Hz), 7.21 (t, 2H, *J*₁ = 4.8 Hz, *J*₂ = 4.0 Hz), 4.30 (t, 4H, *J* = 6.4 Hz), 1.30–1.92 (m, 32H), 1.06 (t, 6H, *J* = 6.4 Hz). ¹³C-NMR (400 MHz, CDCl₃). δ (ppm): 14.11, 22.68, 25.92, 29.34, 29.47, 29.59, 29.61, 30.15, 31.89, 75.06, 111.01, 124.74, 128.30, 130.10, 130.56, 151.05, 158.39, 160.57. Anal. Calcd. for C₃₆H₄₈N₄O₄S₃: C, 62.04; H, 6.94; N, 8.04; S, 13.80. Found: C, 62.10; H, 7.06; N, 7.90; S, 13.97.

2,2¹-(3,4-Ditetradecyloxythiophene-2,5-diyl)bis[5-(2-thienyl)-1,3,4-oxadiazole] (4c)

Yield: 80%, IR (cm⁻¹): 2920, 2851, 2763, 1593 (–C=N), 1463, 1057. FABHRMS: *m/z*, 809. ¹H-NMR (400 MHz, CDCl₃). δ (ppm): 7.85 (d, 2H, *J* = 3.1 Hz), 7.61 (d, 2H, *J* = 4.6 Hz), 7.23 (t, 2H, *J*₁ = 3.9 Hz, *J*₂ = 4.2 Hz), 4.32 (t, 4H, *J* = 6.4 Hz), 1.26–1.91 (m, 48H), 0.89 (t, 6H, *J* = 6.2 Hz). Anal. Calcd. for C₄₄H₆₄N₄O₄S₃: C, 65.31; H, 7.97; N, 6.92; S, 11.89. Found: C, 65.42; H, 7.88; N, 6.75; S, 12.05.

Synthesis of polymers (P1–P3)

To a stirred solution of four equivalents of anhydrous ferric chloride in 20 mL of chloroform, the 1 equivalent of monomer (4a–c) in 10 mL of chloroform was added slowly for 30 min. The reaction mixture was heated to 65–70°C for 24 h. The completion of the reaction was monitored by TLC. After the completion of the reaction, the chloroform was removed by rotary evaporator under vacuum. The solid product obtained was washed with excess of methanol to remove the ferric chloride. The polymers were further purified by Soxhlet extraction technique using methanol as solvent. The polymers were obtained as black powder.



Scheme 1 Synthesis of polymers.

Poly{2,2¹-(3,4- dibutyloxythiophene-2,5-diyyl)
 bis[5-(2-thienyl)-1,3,4-oxadiazole]} (P1)

Yield: 50%, IR (cm⁻¹), 2900, 2840, 2642, 1575 (—C=N—), 1488, 1213. ¹H-NMR (400 MHz, DMSO-*d*⁶). δ (ppm): δ (ppm): 7.72 (d, 2H, *J* = 3.9 Hz), 7.20 (d, 2H, *J* = 4.3 Hz), 4.22 (t, 4H, *J* = 6.7 Hz), 1.22–1.85 (m, 8H), 0.99 (t, 6H, *J* = 6.9 Hz). Anal. Calcd. for C₂₄H₂₂N₄O₄S₃: C, 54.73; H, 4.21; N, 10.64; S, 18.27. Found: C, 54.32; H, 4.00; N, 8.10; S, 18.57. Molecular weight, *M*_w = 3970, *M*_n = 2790, Polydispersity (PD): 1.42.

Poly{2,2¹-(3,4- didecyloxythiophene-2,5-diyyl)
 bis[5-(2-thienyl)-1,3,4-oxadiazole]} (P2)

Yield: 65%, IR (cm⁻¹), 2925, 2859, 2634, 1593 (—C=N—), 1495, 1232. ¹H-NMR (400 MHz, DMSO-*d*⁶). δ (ppm): δ (ppm): 7.82 (d, 2H, *J* = 4.0 Hz), 7.30 (d, 2H, *J* = 4.4 Hz), 4.28 (t, 4H, *J* = 6.5 Hz), 1.32–1.95 (m, 32H), 1.02 (t, 6H, *J* = 6.8 Hz). Anal. Calcd. for C₃₆H₄₆N₄O₄S₃: C, 62.22; H, 6.67; N, 8.06; S, 13.84. Found: C, 62.59; H, 6.32; N, 8.35; S, 14.06. Molecular weight, *M*_w = 3220, *M*_n = 2300, Polydispersity (PD): 1.40.

Poly{2,2¹-(3,4-ditetradecyloxythiophene-2,5-diyyl)
 bis[5-(2-thienyl)-1,3,4-oxadiazole]} (P3)

Yield: 65%, IR (cm⁻¹), 2923, 2853, 2768, 1597 (—C=N—), 1494, 1240. ¹H-NMR (400 MHz, DMSO-*d*⁶). δ (ppm): 7.82 (d, 2H, *J* = 3.6 Hz), 7.22 (d, 2H, *J* = 4.0), 4.30 (t, 4H, *J* = 6.7 Hz), 1.20–1.95 (m, 48H), 0.95 (t, 6H, *J* = 6.4 Hz). Anal. Calcd. for C₄₄H₆₂N₄O₄S₃: C, 65.47; H, 7.74; N, 6.94; S, 11.92. Found: C, 65.12; H, 7.88; N, 7.09; S, 12.18. Molecular weight, *M*_w = 3528, *M*_n = 2433, Poly dispersity (PD): 1.45.

RESULTS AND DISCUSSION

Synthesis and characterization of polymers

Scheme 1 shows the synthetic route for the preparation of monomers and polymers. The required 3,4-ditetradecyloxythiophene-2,5-carboxyhydrazides (**1a,c**) were synthesized by refluxing diethyl 3,4-dialkyloxythiophene-2,5-dicarboxylates with hydrazine monohydrate in methanol. These carboxyhydrazides were condensed with thiophene-2-carbonyl chloride to get the corresponding dicarbohydrazides (**3a,c**), which on treatment with phosphorous oxychloride afforded bis-oxadiazoles (**4a,c**). These monomers were polymerized via chemical polymerization route using anhydrous ferric chloride as polymerization catalyst. The structures of newly synthesized compounds were confirmed by their FTIR, ¹H, ¹³C-NMR, Mass spectral, and elemental analyses.

Formation of 3,4-ditetradecyloxythiophene-2,5-carboxyhydrazide (**1c**) from the corresponding diester was evidenced by its IR and ¹H-NMR spectral data. Its IR spectrum showed sharp peaks at 3290 and 1660 cm⁻¹ indicating the presence of —NH₂ and >C=O groups, respectively. ¹H-NMR spectrum of it displayed peaks at δ 8.34 (s, 2H) and δ 4.98 (s, 4H) for >NH and —NH₂ protons, respectively. Conversion of bishydrazide **1b** to biscarbohydrazide **3b** was confirmed by its IR, ¹H-NMR, and Mass spectral studies. Its IR spectrum exhibited sharp peaks at 3228 and 1715 cm⁻¹ for >NH and >C=O groups, respectively. ¹H-NMR spectrum of it showed (Fig. 3) two >NH protons as singlet at δ values 10.12 and 9.91, thiophene protons as two doublets at δ 7.71 and 7.47, and a triplet at δ 7.04. Its mass spectrum displayed the molecular ion peak at *m/z* 732. Cyclization of biscarbohydrazide **3b** to form bis-oxadiazole **4b** was established by its IR, ¹H-NMR, and Mass spectral data. Its IR spectrum showed no absorption

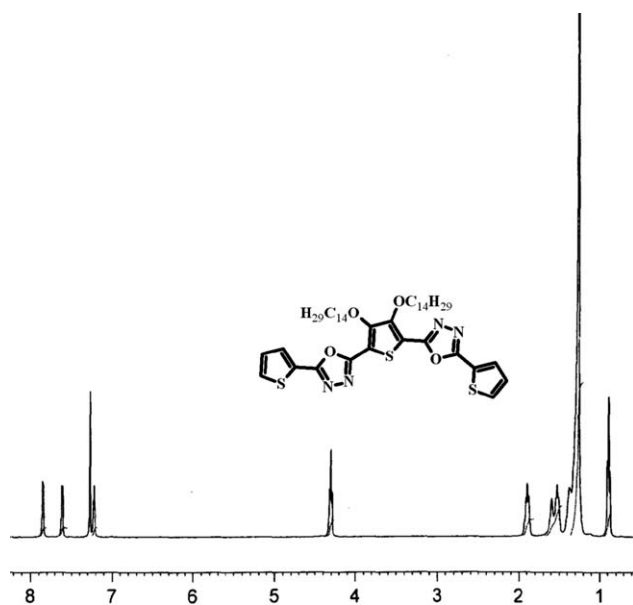


Figure 3 $^1\text{H-NMR}$ spectrum of bis-oxadiazole **4c**.

peaks due to $>\text{NH}$ and $>\text{C}=\text{O}$ groups and appearance of sharp peak at 1593 cm^{-1} indicating the formation of oxadiazole ring. Further, in its $^1\text{H-NMR}$ spectrum, disappearance of two singlets corresponding to $>\text{NH}$ protons confirmed the cyclization.

Finally, polymerization of **4b** to **P2** was established by its IR, $^1\text{H-NMR}$, GPC, and elemental analyses. IR spectrum of **P2** showed characteristic absorption peaks at $2925, 2859\text{ cm}^{-1}$ (C–H stretching aliphatic segments), 1593 cm^{-1} (1,3,4-oxadiazole), 1232 cm^{-1} (C–O–C stretching of ether bond), 1495 cm^{-1} (aromatic). The $^1\text{H-NMR}$ spectra of the polymers in CDCl_3 displayed two doublets δ 7.82 and 7.30, which are due to two thiophene protons. Disappearance of one doublet and conversion of a triplet peak into doublet in the aromatic region clearly confirmed the polymerization of the monomer (**4b**). Further, four protons of $-\text{OCH}_2$ groups attached to thiophene ring resonated at δ 4.28 as triplet. In addition, multiplet peaks were observed in the range δ 1.95–1.42 due to $-(\text{CH}_2)_n-$ protons of alkoxy group. The number and weight average molecular weights of THF soluble part of the polymer **P2** were found to be 2300 and 3220, respectively. Its polydispersity is 1.40.

Electrochemical properties

Cyclic voltametry (CV) was employed to determine redox potentials of new polymers and then to estimate the HOMO and LUMO energy of the polymers, which are of importance to determine the band gap. The cyclic voltammogram of the polymer coated on a glassy carbon electrode was measured on AUTOLAB PGSTAT 30 electrochemical analyzer, using a Pt counter electrode and a Ag/AgCl reference electrode, immersed in the electrolyte $[0.1\text{M } (n\text{-Bu})_4\text{NClO}_4$ in acetonitrile] at a scan rate of 25 mV/S . Electrochemical data of **P1**, **P2**, and **P3** are summarized in Table I.

While sweeping cathodically (Fig. 4), the polymers showed reduction peak at around -1.3 V . These reduction potentials are lower than those of 2-(4-*tert*-butyl phenyl)-1, 3,4-oxadiazole (PBD),^{21,22} one of the most widely used electron transporting materials. In the anodic sweep (Fig. 4), polymers showed oxidation peak at about 1.25 V , comparable with some donor–acceptor type of polymers containing oxadiazole moieties.^{15,16} The onset potentials of *n*- and *p*-doping processes can be used to estimate the HOMO and LUMO of the polymers. The equations reported by de Leeuw et al.,²³ $E_{\text{HOMO}} = -[E_{\text{onset}}^{\text{oxd}} + 4.4\text{eV}]$ and $E_{\text{LUMO}} = -[E_{\text{onset}}^{\text{red}} - 4.4\text{eV}]$ where $E_{\text{onset}}^{\text{oxd}}$ and $E_{\text{onset}}^{\text{red}}$ are the onset potentials versus SCE for the oxidation and reduction of these polymers.

The HOMO energy levels of these polymers were estimated to be $-5.52, -5.59,$ and -5.56 eV , respectively, for **P1**, **P2**, and **P3**. The HOMO energy levels are comparable with CN-PPV and some reported polyoxadiazoles.^{15,16} The LUMO energy levels are lower than those of PPV and some other conjugated *p*-type conjugated polymers indicating that they are having much better electron transporting property. Further, it has been noticed that values are lower than some reported polyoxadiazoles,^{15,16} showing that these polymers possess better electron injection ability. This may be due to the introduction of additional electron withdrawing thiophene rings within the polymer backbone. The very high electron affinities of these polymers may be attributed to the incorporation of electron deficient oxadiazole ring in the polymer backbone. From the onset potentials of oxidation and reduction process, the band gaps of these polymers are estimated to be 2.03, 2.09, and

TABLE I
Electrochemical, Potential, and Energy Levels of the Polymers **P1**, **P2**, and **P3**

Polymer	E_{oxd}	E_{red}	E_{oxd} (onset)	E_{red} (onset)	E_{HOMO} (eV)	E_{LUMO} (eV)	E_g (eV)
P1	1.42	-1.24	1.18	-0.85	5.52	-3.49	2.03
P2	1.20	-1.22	1.25	-0.84	5.59	-3.50	2.09
P3	1.32	-1.35	1.22	-0.95	5.56	-3.39	2.17

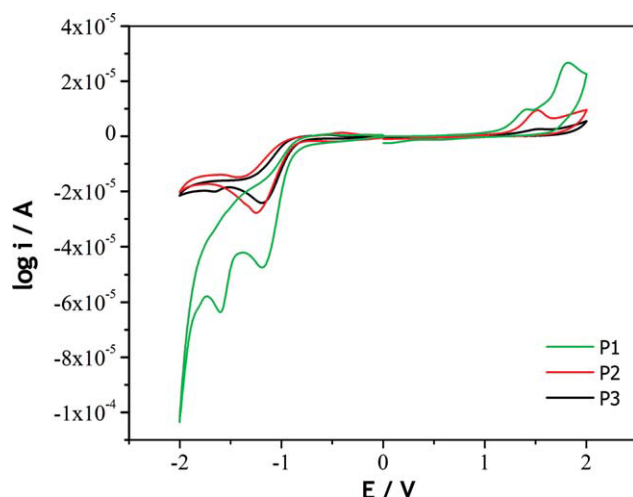


Figure 4 Oxidation and reduction cyclic voltammograms of the polymers. [Color figure can be viewed in the online issue, which is available at www.interscience.wiley.com.]

2.17 for the polymers **P1**, **P2**, and **P3**, respectively. It is clear from the results that improved charge carrying property is expected for the new polymers.

Linear optical properties

The UV-visible absorption and fluorescence spectra of the polymers were recorded in dilute DMF solution. As shown in Figure 5, the absorption maxima of the polymers in dilute DMF solutions are 374, 377, and 375 nm for **P1**, **P2**, and **P3**, respectively. The fluorescence emission spectra of these polymers in solution are shown in Figure 6. The emissive maxima (excitation wavelength 370 nm) of the polymers in dilute DMF solution are 448, 450, and 453 nm for the polymers **P1**, **P2**, and **P3**, respectively. It has been observed that the increase in the length of the

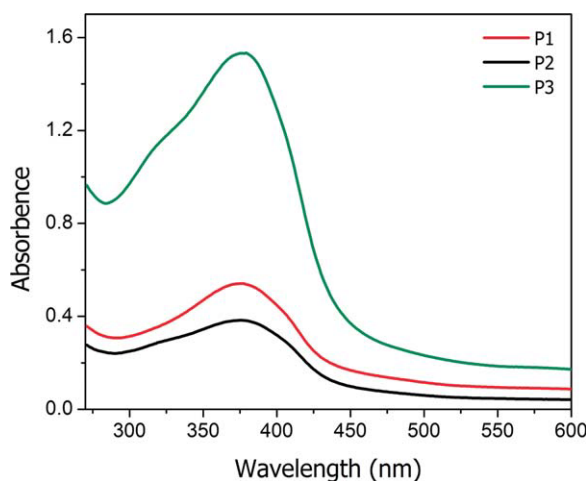


Figure 5 UV-vis absorption spectra of the polymers in DMF solution. [Color figure can be viewed in the online issue, which is available at www.interscience.wiley.com.]

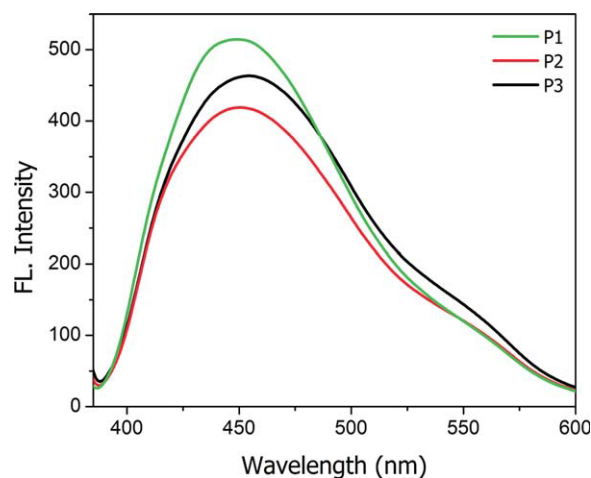


Figure 6 Fluorescence emission spectra of **P1**, **P2**, and **P3** in DMF solution. [Color figure can be viewed in the online issue, which is available at www.interscience.wiley.com.]

alkoxy side chain of the thiophene ring does not show significant change on the optical property. These results indicate that the polymers emit intense bluish-green light by the irradiation of UV light.

Nonlinear optical properties

The linear absorption spectra of the polymers show that the excitation wavelength of 532 nm is close to one of the absorption edges. For the z-scan experiments, the sample concentrations were adjusted such that for each sample the linear transmission was 70% at 532 nm, when taken in a 1 mm cuvette. As shown in Figures 7–9, the polymers **P1**, **P2**, and **P3** shows strong optical limiting behavior, as the transmittance decreases when the pump fluence is increased. It is seen that a 3-photon type absorption (3PA) process gives the best fit to the

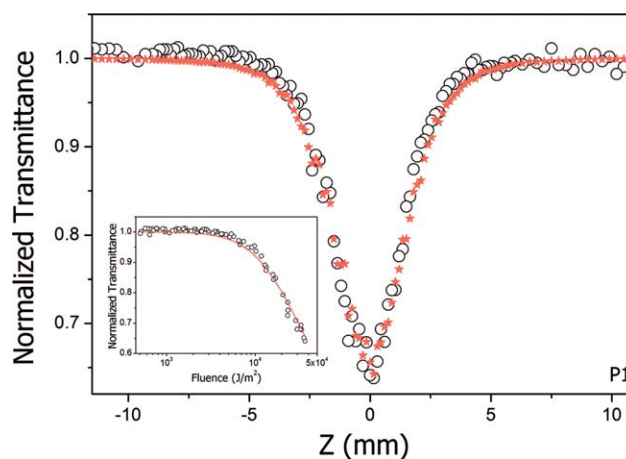


Figure 7 Open aperture z-scan curve for **P1**. [Color figure can be viewed in the online issue, which is available at www.interscience.wiley.com.]

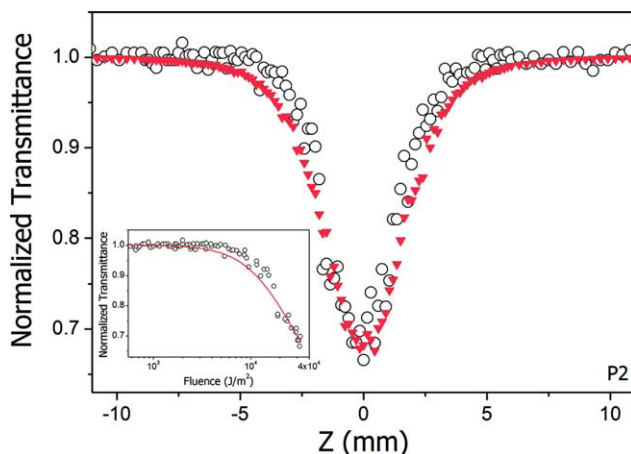


Figure 8 Open aperture z-scan curve for P2. [Color figure can be viewed in the online issue, which is available at www.interscience.wiley.com.]

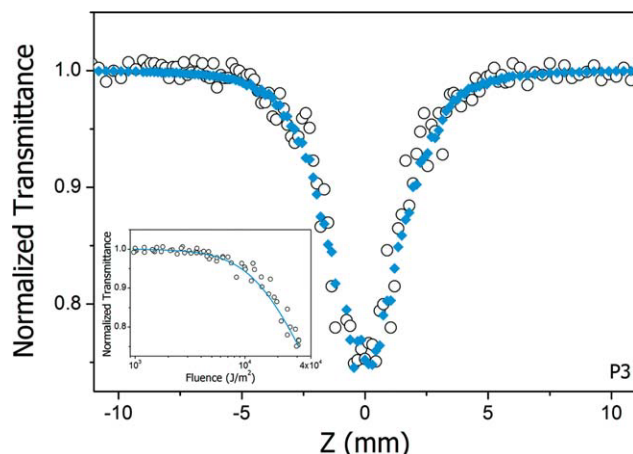


Figure 9 Open aperture z-scan curve for P3. [Color figure can be viewed in the online issue, which is available at www.interscience.wiley.com.]

obtained experimental data. The Z-scan curves obtained are therefore numerically fitted to the nonlinear transmission equation for a three-photon absorption process, given by eq. (1)

$$T = \frac{(1-R)^2 \exp(-\alpha L)}{\sqrt{\pi p_0}} \times \int_{-\infty}^{+\infty} \ln \left[\sqrt{1 + p_0^2 \exp(-2t^2)} + p_0 \exp(-t^2) \right] dt \quad (1)$$

where T is the transmission of the sample. R is the Fresnel reflection coefficient at the sample-air interface, α is the absorption coefficient, and L is the sample length. p_0 is given by $[2\gamma(1-R)^2 I_0^2 L_{\text{eff}}]^2$ where γ is the three-photon absorption coefficient, and I_0 is the incident intensity. L_{eff} is given by $[1 - \exp(-2\alpha L)]/2\alpha$. The 3PA coefficients obtained from the curve fitting are tabulated in Table II. While doing the calculation the pulse-to-pulse energy fluctuations of the laser also are taken into account, and hence the simulated curves are not fully smooth.

Considering the absorption spectra of the samples and recalling that pure three-photon absorption

cross-sections are generally very low, it seems that the observed nonlinearity arises from sequential three-photon absorption involving excited states. Two-photon absorption followed by excited state absorption is another possibility. Therefore, the nonlinearity can be considered as an “effective” three-photon absorption process. In a pure 3PA process, three photons will be simultaneously absorbed and this is an instantaneous nonlinear optical phenomenon. Compared to the usual one-photon absorption process, the cross section for a 3PA is generally low, but they become significant when the samples are irradiated with intense laser pulses of picoseconds or shorter duration. With nanosecond pulse excitation, accumulative nonlinear optical phenomena like excited state absorption and free carrier absorption become more prominent. Depending on the material system under study, excitation wavelength and applied laser fluence, a combination of the instantaneous and accumulative nonlinear effects may take place. These, however, will appear like pure 2PA or pure 3PA in a simple transmission measurement like the z-scan. These combined nonlinearities can hence be termed as “effective 2PA” and “effective 3PA” processes to distinguish them from pure 2PA and

TABLE II
Linear and Nonlinear Optical Parameters for P1, P2, and P3

Linear optical properties		Z-scan		DFWM			
Sample	n^a	α^b (m^{-1})	$\gamma \times (10^{-22} \text{ m}^3/\text{W}^2)$	$\chi^{(3)}$		F	
				$\times (10^{-20} \text{ m}^2/\text{V}^2)$	$\times (10^{-12} \text{ esu})$	$\times (10^{-22} \text{ m}/\text{V}^2)$	$\times (10^{-12} \text{ esu})$
P1	1.4320	71	3.8	2.008	1.437	2.827	2.023
P2	1.4309	71	4	2.213	1.584	3.116	2.231
P3	1.4306	71	2.5	2.194	1.570	3.090	2.211

^a Refractive index.

^b Absorption coefficient.

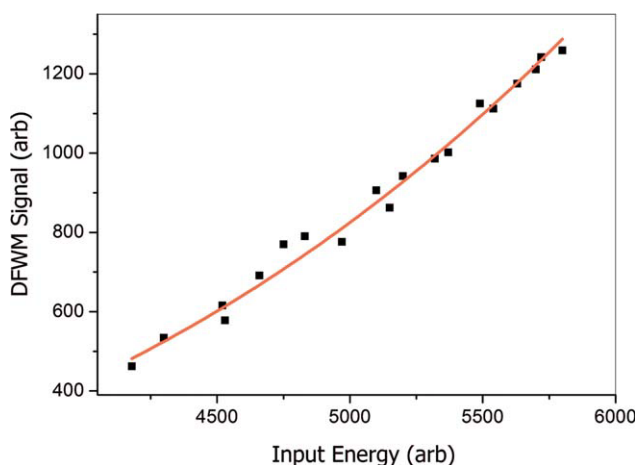


Figure 10 DFWM signal versus input for P1. [Color figure can be viewed in the online issue, which is available at www.interscience.wiley.com.]

3PA processes. During the 3PA process, excitation is proportional to the cube of the incident intensity. This feature may help to obtain higher contrast and resolution in imaging, since 3PA provides a stronger spatial confinement. With the availability of ultrafast pulsed lasers in recent years, significant progress in 3PA-based applications has been witnessed including three-photon pumped lasing and 3PA-based optical limiting and stabilization.²⁴ The high nonlinearity observed in the polymers P1, P2, and P3 may be due to enhanced electron delocalization within the polymer backbone. This is attributed to the presence of additional unsubstituted thiophene rings along the polymer backbone. Such absorptive nonlinearities involving real excited states have been reported earlier in C₆₀, semiconductors, metal nanoclusters, etc.^{25–28}

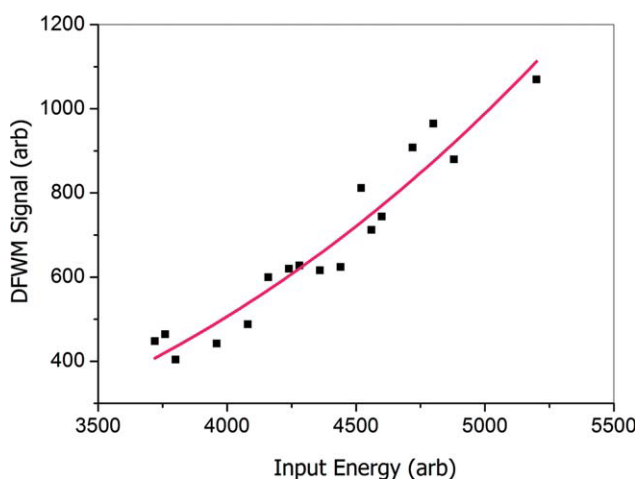


Figure 11 DFWM signal versus input for P2. [Color figure can be viewed in the online issue, which is available at www.interscience.wiley.com.]

DFWM

Variations of the DFWM signal as a function of pump intensity for P1, P2, and P3 are shown in Figures 10–12, respectively. The signal is proportional to cubic power of the input intensity as given by the equation,

$$I(\omega) \propto \left(\frac{\omega}{2\epsilon_0 c n^2} \right) |\chi^{(3)}|^2 l^2 I_0^3(\omega) \quad (2)$$

where, $I(\omega)$ is the DFWM signal intensity, $I_0(\omega)$ is the pump intensity, l is the length of the sample, and n is the refractive index of the medium. The solid curves in the figures are the cubic fits to the experimental data. $\chi^{(3)}$ can be calculated from the equation,

$$\chi^{(3)} = \chi_R^{(3)} \left[\frac{(I/I_0^3)}{(I/I_0^3)_R} \right]^{1/2} \left[\frac{n}{n_R} \right]^2 \frac{l_R}{l} \left(\frac{\alpha l}{(1 - e^{-\alpha l}) e^{-\alpha l/2}} \right) \quad (3)$$

where the subscript R refers to the standard reference, CS₂. " $\chi_R^{(3)}$ " is taken to be $9.5 \times 10^{-21} \text{ m}^2/\text{V}$.²⁷ The figure of merit F , given by $\chi^{(3)}/\alpha$, is then calculated. F is a measure of nonlinear response that can be achieved for a given absorption loss in the medium. The F value is useful for comparing the nonlinearity of different materials when excited in spectral regions of nonzero absorption. Table II shows that the polymers have good F values. The $\chi^{(3)}$ and F values are given in both cgs and SI units. The length of the alkoxy side chains on the 3- and 4-positions of the thiophene ring has not influenced much on the nonlinear optical susceptibility [$\chi^{(3)}$] and figure of merit (F) values.

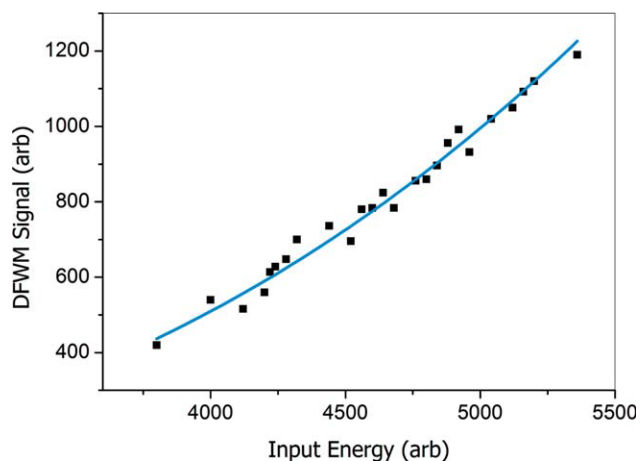


Figure 12 DFWM signal versus input for P3. [Color figure can be viewed in the online issue, which is available at www.interscience.wiley.com.]

CONCLUSIONS

Three new novel conjugated polymers carrying 2,2¹-(3,4-dialkyloxythiophene-2,5-diyl)bis[5-(2-thienyl)-1,3,4-oxadiazole units (**P1**, **P2**, and **P3**) with donor (3,4-dialkoxy thiophene), acceptor (oxadiazole) moiety in the polymer architecture have been successfully prepared by multistep reactions. All the newly synthesized compounds have been characterized. The optical properties revealed that all the polymers emit bluish-green fluorescence under the irradiation of light. The electrochemical properties showed that the polymers **P1**, **P2**, and **P3** possess high-lying HOMO energy levels from -5.52 to -5.59 eV and low lying LUMO levels from -3.39 to -3.50 eV. This is attributed to the presence of alternate donor-acceptor conjugated units along the polymer backbone. The nonlinear optical properties of the polymers have been studied using the Z-scan and DFWM techniques. The polymers showed strong nonlinearity due to "effective" three-photon absorption. Values of the effective three-photon absorption coefficients, third-order nonlinear susceptibilities, and figures of merit have been calculated. The absorptive nonlinearity observed is of the optical limiting type, which can have potential applications.

The authors are grateful to the CDRI, Lucknow, NMR research centre, IISc, Bangalore, and RRL, Trivandrum, for providing instrumental analyses.

References

- Sutherland, R. L. *Handbook of Nonlinear Optics*; Dekker: New York, 1996.
- Perry, J. W.; Mansour, K.; Lee, I.-Y. S.; Wu, X.-L.; Bedworth, P. V.; Chen, C.-T.; Ng, D.; Marder, S. R.; Miles, P.; Wada, T.; Tian, M.; Sasabe, H. *Science* 1996, 273, 1533.
- Ronchi, A.; Cassano, T.; Tommasi, R.; Babudri, F.; Cardone, A.; Farinola, G. M.; Naso, F. *Synth Met* 2003, 139, 831.
- Cassano, T.; Tommasi, R.; Babudri, F.; Cardone, A.; Farinola, G. M.; Naso, F. *Opt Lett* 2002, 27, 2176.
- Burroughes, J. H.; Bradley, D. D. C.; Brown, A. R.; Marks, R. N.; Mackay, K.; Friend, R. H.; Burn, P. L.; Holmes, A. B. *Nature* 1992, 347, 539.
- Grem, G.; Leditzky, G.; Ullrich, B.; Leising, G. *Adv Mater* 1992, 4, 36.
- Leclerc, M. *J Polym Sci Part A: Polym Chem* 2001, 39, 2867.
- Pei, J.; Yu, W.-L.; Haung, W.; Heeger, A. J. *Chem Commun* 2000, 1631.
- Nisoli, M.; Cybo-Ottone, A.; De Silvestri, S.; Magni, V.; Tubino, R.; Botta, C.; Musco, A. *Phys Rev B* 1993, 47, 10881.
- Roncali, J. *Chem Rev* 1992, 92, 711.
- Kishino, S.; Ueno, Y.; Ochiai, K.; Rikukawa, M.; Sanui, K.; Kobayashi, T.; Kunugita, H.; Ema, K. *Phys Rev B* 1998, 54, 430.
- Udayakumar, D.; John Kiran, A.; Adhikari, A. V.; Chandrasekharan, K.; Shashikala, H. D. *J Appl Polym Sci* 2007, 106, 3033.
- Udayakumar, D.; John Kiran, A.; Adhikari, A. V.; Chandrasekharan, K.; Umesh, G.; Shashikala, H. D. *Chem Phys* 2006, 331, 125.
- John Kiran, A.; Udayakumar, D.; Chandrasekharan, K.; Adhikari, A. V.; Shashikala, H. D. *J Phys B: At Mol Opt Phys* 2006, 39, 3747.
- Udayakumar, D.; Adhikari, A. V. *Synth Met* 2006, 156, 1168.
- Udayakumar, D.; Adhikari, A. V. *Opt Mater* 2007, 29, 1710.
- Overberger, C. G.; Lal, J. *J Am Chem Soc* 1951, 73, 2956.
- Daoust, G.; Leclerc, M. *Macromolecules* 1991, 24, 455.
- Zhong, Q. T.; Tour, J. M. *J Am Chem Soc* 1998, 120, 5355.
- Sheik-Bahae, M.; Said, A. A.; Wei, T.; Hagan, D. J.; Van Styland, E. W. *IEEE J Quantum Electron* 1990, 26, 760.
- Strukelj, M.; Papadimitrakopoulos, F.; Miller, T. M.; Rotheberg, L. J. *Science* 1995, 267, 1969.
- Janietz, S.; Wedel, A. *Adv Mater* 1997, 9, 403.
- De Leeuw, D. M.; Simenon, M. M. J.; Brown, A. B.; Einerhand, R. E. F. *Synth Met* 1997, 84, 53.
- Qingdong, Z.; Guang He, S.; Changgui, L.; Prasad, P. N. *J Mater Chem* 2005, 15, 3488.
- Harilal, S. S.; Bindhu, C. V.; Nampoori, V. P. N.; Vallabhan, C. P. G. *J Appl Phys* 1999, 86, 1388.
- Tutt, L. W.; Boggess, T. F. *Prog Quantum Electron* 1993, 17, 299.
- Philip, R.; Ravindrakumar, G.; Sandhyarani, N.; Pradeep, T. *Phys Rev B* 2000, 62, 13160.
- Wang, P.; Ming, H.; Xie, J.; Zhang, W.; Gao, X.; Xu, Z.; Wei, X. *Opt Commun* 2001, 192, 387.